International Journal on Science and Technology (IJSAT)
E-ISSN: 2229-7677 ● Website: www.ijsat.org ● Email: editor@ijsat.org

Self-similar dynamics of a cylindrical shock wave in a rotating, self-gravitating dusty gas under monochromatic radiation

Gyanendra Kumar Chaudhary[1], Arvind Kumar Singh[2]

[1]Department of Mathematics and Statistics D.D.U. Gorakhpur University, Gorakhpur, INDIA.

Abstract:
The study explores the propagation of a cylindrical shock wave in a self-gravitating, rotat- ing axisymmetric dusty gas subjected to monochromatic radiation of constant intensity per unit area. The gas is considered grey and opaque, while the shock wave itself is transparent. The fluid velocity has variable azimuthal and axial components. The dusty gas is modeled as a mixture of a non-ideal gas and small solid particles, which are continuously distributed throughout. To capture key characteristics of shock propagation, the solid particles are treated as a pseudo-fluid, ensuring that equilibrium flow conditions are maintained across the entire flow field. Similarity solutions are derived, and the influence of various parame- ters—such as radiation, gravitation, gas non-idealness, mass concentration of solid particles, and the density ratio of solid particles to the initial gas density—is analyzed in detail. The similarity solution holds under the assumption of a constant initial angular velocity, and it is observed that shock strength remains unaffected by both the radiation and gravitation parameters. Additionally, the radiation parameter plays a dominant role in governing the effect of dusty gas parameters on radiation heat flux variation. Furthermore, the total en- ergy in the flow field behind the shock front is not conserved but instead varies as the fourth power of the shock radius.

1. Introduction

Shock processes occur in various astrophysical scenarios, including supernova explosions, pho-toionized gas regions, stellar winds, and collisions between high-velocity clumps of interstellar gas. These phenomena play a crucial role in astrophysics and space sciences. For instance, a global shock wave can result from a stellar pulsation or a supernova explosion propagating outward through a stellar envelope. Similarly, shocks may arise from point sources, such as man-made explosions in Earth's atmosphere or impulsive flares in the Sun's atmosphere. Shock waves are widespread throughout the observable universe and serve as key mechanisms for energy transport into the inter-stellar medium, initiating processes observed in nebulae that can ultimately lead to star formation. The interstellar medium frequently experiences shock waves due to numerous supersonic motions

* maths.gkc93@yahoo.com
† dr.arvindsingh1980@gmail.com

and energetic events, including supernova explosions, cloud-cloud collisions, bipolar outflows from young protostellar objects, and powerful mass loss from massive stars in their late evolutionary stages (stellar winds). Additionally, shock waves are associated with spiral density waves, radio galaxies, and quasars. Similar phenomena also occur in laboratory settings, such as when a piston rapidly moves through a tube of gas (shock tube), a projectile or aircraft travels supersonically through the atmosphere, a strong explosion generates a blast wave, or when rapidly flowing gas encounters a constriction in a flow channel or impacts a solid boundary.

The study of shock waves in a mixture of small solid particles and gas is significant due to its broad applications in various fields, including lunar ash flow, coal-mine blasts, nozzle flow, bomb blasts, metallized propellant rocket blasts, underground and volcanic explosions, supersonic flight in polluted air, planetary collisions with cometary comas, star formation, particle acceleration in shocks, and the formation of dusty crystals, among others [1–5]. Recently, research on dusty-gas flow has garnered attention due to its implications for environmental and industrial issues. When a moving shock wave interacts with a two-phase medium consisting of gas and particles, a flow-field develops with significant practical applications, such as in solid rocket engines, where aluminum particles reduce vibrations caused by instability, and in industrial accidents like explosions in coal mines and grain elevators [6].

Miura and Glass [3] provided an analytical solution for a planar shock wave in a dusty gas under constant velocity conditions. Since the volume occupied by solid particles mixed into a perfect gas is negligible, the dust primarily contributes to the mass fraction rather than the volume fraction. Their results highlight the impact of the additional inertia of dust on shock propagation. Furthermore, Pai et al. [1] extended the classical strong explosion solution—resulting from the instantaneous release of energy in a gas—to a two-phase flow system comprising a mixture of small solid particles and a perfect gas. Their findings elucidate the key effects of dust particles on strong shock waves. As they accounted for a nonzero volume fraction of solid particles, their results demonstrate how the presence of dust reduces the mixture's compressibility while increasing its inertia, ultimately affecting shock wave propagation. Higashino and Suzuki [2] investigated line-source explosions in a dusty gas, assuming velocity and temperature equilibrium. Meanwhile, Steiner and Hirschler [7] derived analytical solutions for the one-dimensional, unsteady, self-similar flow of a dusty gas between a strong shock and a moving piston. Their results suggest that the inertia of dust particles and the behavior of the solid phase significantly influence wave propagation dynamics.

In recent years, significant focus has been placed on examining the interaction between gasdynamics and radiation. When radiation effects are incorporated into gasdynamics, the fundamental non-linear equations become increasingly complex. Consequently, it becomes imperative to develop approximations that maintain physical accuracy while facilitating substantial simplifications. The study of radiation-gas dynamics interactions has been explored by various researchers using the theory of dimensionality pioneered by Sedov [8].

Marshak [9] derived similarity solutions for radiation hydrodynamic equations under specific conditions, such as plane symmetry, where radiation flux plays a crucial role, though radiation pressure and energy remain negligible. He analyzed cases involving (1) constant density, (2) constant pressure, and (3) temperature variations following a power-law dependence over time. Elliott

[10] investigated the conditions necessary for self-similarity by defining a particular functional form for the mean-free path of radiation.

Several studies have explored scenarios involving stationary or moving radiating walls that generate shocks at the leading edge of self-similar flow fields. Notable contributions include the works of Wang [11], Helliwell [12], and Nicastro [13]. Ray and Bhowmick [14] formulated self-similar solutions for central stellar explosions, incorporating radiation flux under the assumption of an isothermal and transparent shock. Khudyakov [15] investigated self-similar gas motion influenced by monochromatic radiation, while Zheltukhin [16] developed a family of exact solutions describing one-dimensional motion—whether plane, cylindrical, or spherical—of a perfect gas considering monochromatic radiation absorption.

Further developments in this domain include the work of Vishwakarma and Pandey [20], who analyzed one-dimensional flow behind a cylindrical magnetogasdynamic shock wave propagating in a non-ideal gas under monochromatic radiation influence. Expanding on this, Nath, Sahu, and Dutta [21] studied magnetohydrodynamic cylindrical shock waves in a non-uniform, rotating, non-ideal gas under monochromatic radiation. Additionally, Nath and Sahu [22] examined cylindrical shock waves in a rotational axisymmetric non-ideal gas subjected to monochromatic radiation effects, later extending their research to explore shock wave behavior in a non-ideal dusty gas under similar conditions [24].

Sahu [25] further investigated the propagation of cylindrical shock waves in a rotational axisymmetric non-ideal gas under monochromatic radiation while accounting for an increasing energy profile, incorporating variable azimuthal and axial fluid velocities. Collectively, these studies enhance our understanding of gas-radiation interactions, offering valuable insights into astrophysical and high-energy environments.

The study of significant celestial phenomena must focus on understanding the motion of gaseous masses influenced by shock waves in a gravitational field. Gravitational forces play a crucial role in various astrophysical scenarios, affecting dynamic processes in stellar and interstellar environments. The rapid release of energy following the unsteady motion of a massive gas cloud can lead to flare- ups in novae and supernovae. The behavior of such gaseous masses can be analyzed using the equations of motion and equilibrium, incorporating the effects of gravitational forces.

Carrus et al. [26] employed numerical methods to derive similarity solutions for the propagation of shock waves in a gas subjected to the gravitational attraction of a central fixed-mass body, known as the Roche model. Similarly, Rogers [27] proposed an analytical method to address the same problem. Patel [28] extended the investigation by obtaining self-similar solutions for the one-dimensional unsteady adiabatic flow of a dusty gas behind a spherical shock wave within a gravitational field. Recent studies have further explored self-similar solutions for shock waves in various media, including perfect gases, non-ideal gases, and dusty gases, under gravitational influences [29–31].

Despite these contributions, none of the aforementioned studies have examined the impact of the gravitational field on shock wave propagation in a rotating axisymmetric non-ideal dusty gas under monochromatic radiation. The role of small solid particles in the presence of both monochromatic radiation and a gravitational field remains largely unexplored. In this study, we extend the work of Nath and Thakar on perfect gases by considering a dusty gas—a combination of a non-ideal gas

and fine solid particles—while incorporating the effects of the gravitational field, medium rotation, and the components of the vorticity vector through a slightly modified transformation.

This study aims to derive self-similar solutions for the flow behind a cylindrical shock wave propagating through a rotating, axisymmetric, non-ideal dusty gas under the influence of monochromatic radiation and a gravitational field. The fluid exhibits variable axial and azimuthal velocities in the ambient medium, following power-law distributions. A constant-intensity radiation flux (j_0) is assumed to move in the direction opposite to the shock wave's propagation. The gas it- self is considered non-radiating, with radiation absorption occurring solely behind the shock front. Additionally, the gas is treated as gray and opaque, while the shock wave is transparent.

The shock propagates through a conducting medium initially at rest. To capture key characteristics of shock propagation, small solid particles are modeled as a pseudo-fluid, forming a mixture in thermal and velocity equilibrium with a constant specific heat ratio. The effects of thermal conductivity and viscous stress in this mixture are considered negligible. This study examines how variations in the gas's non-idealness parameter, the ratio of solid particle density to the gas's initial density, the mass concentration of solid particles, the radiation parameter, and the gravitational parameter influence the shock wave dynamics.

1. Equations of Motion and Boundary Conditions

The fundamental equations for one-dimensional unsteady adiabatic flow behind a shock wave in a self-gravitating, rotating axisymmetric dusty gas (mixture of a non-ideal gas and small solid particles) under the action of monochromatic radiation, neglecting heat-conduction, viscosity, and radiation of the medium, can be presented in the Eulerian coordinates in the following form [1, 15, 17, 30–33]:

$$\frac{\partial \rho}{\partial t} + u\frac{\partial \rho}{\partial r} + \rho\frac{\partial u}{\partial r} + \frac{u\rho}{r} = 0, \tag{1}$$

$$\frac{\partial u}{\partial t} + u\frac{\partial u}{\partial r} + \frac{1}{\rho}\frac{\partial \rho}{\partial r} + \frac{Gm}{r} - \frac{v^2}{r} = 0, \tag{2}$$

$$\frac{\partial v}{\partial t} + u\frac{\partial v}{\partial r} + \frac{uv}{r} = 0, \tag{3}$$

$$\frac{\partial w}{\partial t} + u\frac{\partial w}{\partial r} = 0, \tag{4}$$

$$\frac{\partial m}{\partial t} = 2\pi\rho r = 0 \tag{5}$$

$$\frac{\partial U_m}{\partial t} + u\frac{\partial U_m}{\partial t} - \frac{P}{\rho^2}\left(\frac{\partial \rho}{\partial t} + u\frac{\partial \rho}{\partial r}\right) = \frac{1}{\rho r}\frac{\partial (Fr)}{\partial r}, \tag{6}$$

$$\frac{\partial F}{\partial r} = KF, \tag{7}$$

where r and t are the independent space and time coordinates, u, v and w are the radial, azimuthal and axial components of the fluid velocity $\vec{q}$ in the cylindrical coordinates (r, θ, z), F is the flux of monochromatic radiation per unit area at a radial distance r and time t, K is the absorption coefficient, $\bar{G}$ is the gravitational constant, and p, ρ, m and U_m are the pressure, density, total mass per unit volume and internal energy per unit mass of the mixture.

Also,

$$v = \omega r, \tag{8}$$

where 'ω' is the angular velocity of the medium at radial distance r from the axis of symmetry. In this case the vorticity vector $\zeta = \frac{1}{2} curl\, \vec{q}$, has the following components

$$\zeta_r = 0,\ \zeta_\theta = -\frac{1}{2}\frac{\partial w}{\partial r},\ \zeta_z = \frac{1}{2r}\frac{\partial}{\partial r}(rv) \tag{9}$$

To introduce a new parameterized form of the equation of state for the non-ideal gas in the dusty gas mixture, we redefine the internal volume parameter b and introduce a generalized compressibility function $f(\rho_g)$ to account for non-ideal effects. The equation of state then takes the form:

$$p_g = R^*\rho_g f(\rho_g)T, \tag{10}$$

where $f(\rho_g)$ is a function that modifies the ideal gas law to accommodate non-ideal behavior. A commonly used form that retains the original structure while introducing a new parameter B is:

$$f(\rho_g) = 1 + B\rho_g^n.$$

Thus, the new parameterized equation of state becomes:

$$p_g = R^*\rho_g(1 + B\rho_g^n)T.$$

B is a modified non-ideality parameter that generalizes the internal volume effect. n is an exponent that controls the non-linearity of the density dependence. This form allows for greater flexibility in modeling real gas behavior, where different values of B and n can be used to fit experimental data more accurately.

To account for the behavior of solid particles in the mixture, we assume that their specific volume remains constant, unaffected by changes in temperature and pressure. Consequently, the equation governing the state of the solid particles can be expressed in a more generalized parameterized form as

$$\rho_{sp} = \rho_{sp,0} f(K_p, T, p),$$

where ρ_{sp} represents the specific density of the solid particles, $\rho_{sp,0}$ is a reference density, and $f(K_p, T, p)$ is a function that characterizes the dependence of density on the mass concentration of solid particles K_p, temperature T, and pressure p.

Under the assumption that the specific volume remains unchanged, we set f(K_p, T, p) = 1, leading to

$$\rho_{sp} = \rho_{sp,0} = \text{constant}. \tag{11}$$

This formulation ensures that the density of the solid particles remains independent of thermo- dynamic variations within the mixture. The equation of state of the mixture of a non-ideal gas and small solid particles can be written as given below [34, 35]

$$p = \frac{(1-K_p)}{(1-Z)}\left[1 + b\left(1 - K_p\right)\rho\right]\rho R^* T. \tag{12}$$

Here $K_p = \frac{m_{sp}}{m}$ is the mass fraction of solid particles, $Z = \frac{V_{sp}}{V_m}$is the volume fraction of solid particles in the mixture, m_{sp} and V_{sp} are the total mass and volume of the solid particles, respectively, V_m is the total volume of the mixture.

The internal energy per unit mass of the mixture can be written as

$$U_m = \frac{p(1 - Z)}{(\Gamma - 1)\,\rho[1 + b\rho(1 - K\ )]\dot{\rho}} \tag{13}$$

where Γ is the ratio of the specific heats of the mixture.

The absorption coefficient K is considered to vary as [15, 17, 18]

$$K = K_0 \rho^{\alpha} p^{\delta} F^{\,q} r^{s} t^{l}, \tag{14}$$

where K_0 (the coefficient of radiation absorption ahead of the shock wave front) is a dimensional constant, and the exponents α, δ, q, s and l are rational numbers.

We assume that a diverging cylindrical shock wave is propagating in the dusty gas with a constant density. Therefore, the following equalities are valid for the flow variables immediately ahead of the shock front:

$$u = u_a = 0, \tag{15}$$

$$\rho = \rho_a = \text{constant}, \tag{16}$$

$$v = v_a = v^* R^{\lambda}, \tag{17}$$

$$w = w_a = w^* R^{\sigma}, \tag{18}$$

where v^*, w^*, λ and σ are constants, R is the shock radius, and the subscript 'a' refers to the conditions immediately ahead of the shock front.

In the undisturbed state of the gas, the equation (2) and (3) gives

$$m_a = \pi \rho_a R, \tag{19}$$

$$p_a = \frac{-\bar{G}\pi\rho_a^2 R^2}{2} + \frac{\rho_a v^{*2} R^{2\lambda}}{2\lambda} \tag{20}$$

The components of the vorticity vector ahead of the shock vary as

$$\zeta_{r_a} = 0,\ \zeta_{\theta_a} = -\frac{w^*\sigma}{2}R^{\sigma-1}, \zeta_{z_a} = \frac{(1+\lambda)v^*}{2}\mathrm{R}^{\lambda-1} \tag{21}$$

From equations (8) and (17), the initial angular velocity of the ambient medium vary as

$$\omega_a = v^* R^{\lambda-1}. \tag{22}$$

The jump conditions at the shock propagating into non-ideal dusty gas which is transparent for the radiation flux, are given by the conservation of mass, momentum and energy across the shock

$$\rho_a \dot{\mathrm{R}} = \rho_n(\dot{\mathrm{R}} - \mathrm{u}_n), \tag{23}$$

$$\mathrm{p}_a + \rho_a \dot{\mathrm{R}}^2 = \mathrm{p}_n + \rho_n(\dot{\mathrm{R}} - \mathrm{u}_n)^2, \tag{24}$$

$$U_{m_a} + \frac{p_a}{\rho_a} + \frac{\dot{R}^2}{2} = U_{m_n} + \frac{p_n}{\rho_n} + \frac{(\dot{R}-u_n)^2}{2} \tag{25}$$

$$\frac{Z_a}{\rho_a} = \frac{Z_n}{\rho_n}, \tag{26}$$

$$\mathrm{F}_a = \mathrm{F}_n, \tag{27}$$

$$\mathrm{m}_a = \mathrm{m}_n, \tag{28}$$

$$\mathrm{v}_a = \mathrm{v}_n, \tag{29}$$

$$\mathrm{w}_a = \mathrm{w}_n, \tag{30}$$

where the subscript ‘n’ denotes the conditions immediately behind the shock front, $\dot{R} = \frac{dR}{dt}$ denotes the velocity of shock front.

From equation (15), the flow variables behind the shock front are given by

$$\rho_n = \frac{\rho_a}{\beta}, \tag{31}$$

$$u_n = (1-\beta)\dot{R} \tag{32}$$

$$p_n = \rho_a\ \dot{R}^2\left[(1-\beta) + \frac{1}{\gamma M^2}\right], \tag{33}$$

$$Z_n = \frac{Z_a}{\beta} \tag{34}$$

$$\mathrm{F}_n = \mathrm{F}_a, \tag{35}$$

$$\mathrm{m}_n = \mathrm{m}_a, \tag{36}$$

$$\mathrm{v}_n = \mathrm{v}_a, \tag{37}$$

$$\mathrm{w}_n = \mathrm{w}_a, \tag{38}$$

where $\mathrm{M}^2 = (\frac{\rho_a \dot{R}^2}{\gamma P_a})^{1/2}$ is the shock-Mach number referred to the frozen speed of sound $(\frac{\gamma P_a}{\rho_a})^{1/2}$

The quantity β (0 < β < 1) is obtained by the relation

$$\beta^2\left(\frac{\Gamma+1}{2}\right) - \beta\left[\frac{\Gamma}{\gamma M^2} + \left(\frac{\Gamma-1}{2}\right)\{1+\bar{b}(1-K_p)\} + Z_a - (\Gamma-1)\bar{b}(1-K_p)\right] - \left(\frac{\Gamma-1}{2}\right)\bar{b}(1-K_p) - \frac{(\Gamma-Z_a)\bar{b}(1-K_p)+(\Gamma-1)\,\bar{b}^2(1-K_p)^2}{\gamma M^2\{1+\bar{b}(1-K_p)\}} = 0, \tag{39}$$

where Z_a is the initial volume fraction and $\bar{b} = b\rho_a$ is the non-idealness parameter of the gas. Equation (39) gives two different values of β for all the values of parameters Γ, γ, M, $\bar{b}$, K_p and Z_a, out of which only one value lies in the required range 0 < β < 1, i.e. only one value of β satisfies the physical limit of the considered problem.

The jump conditions for the components of vorticity vector across the shock front are given as

$$\zeta_{\theta_n} = \frac{\zeta_{\theta_a}}{\beta}, \qquad \zeta_{z_n} = \frac{\zeta_{z_a}}{\beta} \tag{40}$$

The dimension of the constant coefficient K_0 in equation (14) is calculated as [17, 20]

$$[K0] = M^{-\alpha-\delta-q} L^{3\alpha+\delta-s-1} T^{2\delta+3q} \tag{41}$$

By following the approach of Sedov [8], we get the conditions under which the formulated problem has self similar solutions. The relation between ρ_a, p_a and F_a is given as

$$Fa = pa^{3/2}\rho a^{-1/2}. \tag{42}$$

For the existence of similarity solution, the radiation absorption K_0 must depend on the dimen- sions of F_a and ρ_a, which holds under the condition $s + l = -1$.

2. Similarity Transformations

Zel'dovich and Raizer [36] showed that the gas dynamic equations acknowledge similarity trans-formations, that there are possible different flows similar to each other which are derivable from each other by changing the basic scales of length, time, and density. For self-similar motions, the system of fundamental partial differential equations (1)-(7) reduces to a system of ordinary differential equations in new unknown functions of the similarity variable η which is defined by

$$\eta = \frac{r}{R}, R = R(t) = \bar{\lambda} F_b^{1/\delta} \rho b^{1/\delta} t^K.$$

where $\bar{\lambda}$ is a dimensionless proportionality constant, similar to $\bar{\beta}$, ensuring $\eta = 1$ at the shock surface. F_b is a generalized source strength parameter. ρ_b represents the ambient medium density. δ is a general exponent that determines how F_b and ρ_b contribute to the scaling. κ is an exponent that determines the time dependence of the shock radius.

This formulation allows for more general scaling laws beyond the standard Sedov-Taylor blast wave solution. The value of the constant $\bar{\beta}$ is so chosen that $\eta = 1$ at the shock surface [8].

The velocity, density, pressure, heat flux and length scales are not all independent of each other. If we choose R and ρ_a as the basic scales, then the quantity $\frac{dR}{dT} = \dot{R}$ can serve as the velocity scale, $\rho_a \dot{R}^2$ as the pressure scale. This does not restrict the universality of the solution as a scale is only defined within a numerical coefficient, which can always be involved in the new unknown function. Therefore, we represent the solution of the partial differential equations (1)-(7) in terms of products of scale functions and the new unknown functions of the similarity variable η in the following form [34, 37]

$$u = \dot{R}\ U(\eta), \tag{43}$$

$$v = \dot{R}\ V(\eta), \tag{44}$$

$$w = \dot{R}\ W(\eta), \tag{45}$$

$$\rho = \rho_a D(\eta), \tag{46}$$

$$p = \rho_a \dot{R}^2 P(\eta), \tag{47}$$

$$F = F_a \phi(\eta), \tag{48}$$

$$Z = Z_a D(\eta), \tag{49}$$

$$m = m_a S(\eta), \tag{50}$$

where U, V, W, D, P, ϕ and S are new non-dimensional functions of the similarity variable η. The differential equations are to be formulated in terms of the similarity variable η.

In order to obtain similarity solutions, the Shock Mach number M, which occurs in the shock conditions (31)-(38) must be a constant parameter (i.e. Mach number should be independent of Time). Using equations (16) and (20) into $M = (\frac{\rho_a \dot{R}^2}{\gamma P_a})^{1/2}$, we have obtained the expression for Shock Mach number as

$$M = \frac{2\dot{R}^2}{\gamma\left[\frac{v^{*2}R^{2\lambda}}{\lambda} - \bar{G}\pi P_a R^2\right]} \tag{51}$$

Therefore, Mach number M is constant for

$$\dot{R} = QR; \lambda = 1, \tag{52}$$

and, we obtain a relation for gravitation parameter $G_0 = \frac{\bar{G}\pi P_a}{Q^2}$ as

$$G_0 = \frac{v^{*2}}{Q^2} - \frac{2}{\gamma M^2} \tag{53}$$

The relation (53) is analogous to the relations (103) of Rogers [27] and (20) of Singh [29] for the case of a perfect gas with a variable initial density of the medium, equation (3.7) of Patel [28] for the case of a mixture of perfect gas and small solid particles, equation (55) of Bajargaan and Patel [30] for the case of a mixture of non-ideal gas and small solid particles. The quantity G_0 is a gravitation parameter, which is analogous to the parameter l_1 of Rosenau [38]. The parameter $\frac{v}{Q}$ is similar to the parameter $\frac{B}{Q}$ in relation (66) of Vishwakarma and Nath [39] in the absence of the gravitational field.

By using the similarity transformations (43)-(50), the fundamental system of partial differential equations (1)-(7) reduces into

$$(U - \eta)\frac{dD}{d\eta} + D\frac{dU}{d\eta} + \frac{DU}{\eta} = 0 \tag{54}$$

$$U + (U - \eta)\frac{dU}{d\eta} + \frac{1}{D}\frac{dP}{d\eta} + G_0\frac{S}{\eta} - \frac{V^2}{\eta} = 0, \tag{55}$$

$$(U-\eta)\frac{dV}{d\eta}+V+\frac{UV}{\eta}=0 \tag{56}$$

$$(U-\eta)\frac{dW}{d\eta}+W=0, \tag{57}$$

$$\frac{dS}{d\eta}=2\mathrm{D}\eta, \tag{58}$$

$$2PD(1-Z_aD)\{1+\bar{b}(1-K_p)\}+(U-\eta)\bar{b}PD^2D'\bar{b}(1-K_p)\{Z_a+\bar{b}(1-K_p)\}-\Gamma PD'(U-\eta)\{1+\bar{b}D(1-K_p)\}^2+P'D(U-\eta)(1-Z_aD)\{1+\bar{b}D(1-K_p)\}=\frac{(\Gamma-1)D\{1+\bar{b}\,D(1-K_p)\}^2}{(\eta\gamma^{3/2}M^3)}(\eta\phi'+\phi) \tag{59}$$

$$\phi'=(\gamma M^2)^{\delta}\xi n^S D^{\alpha}P^{\delta}\phi^{q+1} \tag{60}$$

Where

$$\xi=K_0{\rho_a}^{\alpha-\frac{\delta}{3}-q} \tag{61}$$

under the condition 3q + 2δ + s + 1 = 0 for similarity solutions. The quantity ξ is a dimensionless constant taken as the parameter which characterizes the interaction between the gas and the incident radiation flux [15, 17].

The above set of differential equations (54)-(60) can be transformed and simplified into

$$U'=\frac{U}{\eta}-\frac{(U-\eta)D'}{D}, \tag{62}$$

$$D'=\frac{1}{N}[D^2(U-\eta)(1-Z_aD)\left\{U-\frac{(U-\eta)U}{\eta}+G_0\frac{S}{\eta}-\frac{V^2}{\eta}\right\}-2PD(1-Z_aD)\{1+\bar{b}D(1-K_p)\}+\frac{(\Gamma-1)D\{1+\bar{b}D(1-K_p)\}^2\phi}{\eta\gamma^{3/2}M^3}\{(\gamma M^2)^{\delta}\xi n^S D^{\alpha}P^{\delta}\phi^{q+1}\}] \tag{63}$$

$$P'=\frac{(U-\eta)UD}{\eta}-UD+(U-\eta)^2D'-\frac{G_0SD}{\eta}+\frac{V^2D}{\eta} \tag{64}$$

$$V'=-\frac{V}{(U-\eta)}-\frac{UV}{(U-\eta)\eta}\ , \tag{65}$$

$$W'=-\frac{W}{(U-\eta)}, \tag{66}$$

$$S'=2D\eta, \tag{67}$$

$$\phi'=(\gamma M^2)^{\delta}\xi n^S D^{\alpha}P^{\delta}\phi^{q+1} \tag{68}$$

Where $N=(U-\eta)\bar{b}PD^2\bar{b}(1-K_p)\{Z_a+\bar{b}(1-K_p)\}-\Gamma P(U-\eta)\{1+\bar{b}D(1-K_p)\}^2+D(\mathrm{U}-\eta)^3(1-Z_aD)\{1+\bar{b}D(1-K_p)\}$

By using the similarity transformations (43)-(50), the shock conditions (31)-(38) are transformed

into

$$U(1) = (1-\beta), \tag{69}$$

$$D(1) = \frac{1}{\beta}, \tag{70}$$

$$P(1) = (1-\beta) + \frac{1}{\gamma M^2}, \tag{71}$$

$$V(1) = (G_0 + \frac{2}{\gamma M^2})^{1/2} \tag{72}$$

$$W(1) = \frac{w^*}{Q}, \tag{73}$$

$$S(1) = 1, \tag{74}$$

$$\phi(1) = 1, \tag{75}$$

where $\lambda = \sigma = 1$. In addition to shock conditions (69) to (75), the condition which is to be satisfied at the piston surface is that the velocity of the fluid is equal to the velocity of the piston itself. This kinematic condition from equation (43) can be written as

$$U(\eta_p) = \eta_p, \tag{76}$$

where $\eta_p = \frac{u_p}{\dot{R}}$

After Applying the similarity transformation (44), (45) on the equation (9), the non-dimensional components of the vorticity vector $l_r = \frac{\zeta_r}{(\dot{R}/R)}, l_\theta = \frac{\zeta_\theta}{(\dot{R}/R)}, l_{z^*} = \frac{\zeta_z}{(\dot{R}/R)}$ in the flow-field behind the shock front can be written as

$$l_r = 0\,, \tag{77}$$

$$l_\theta = \frac{W}{2(U-\eta)}\,, \tag{78}$$

$$l_{z^*} = -\frac{V}{(U-\eta)}\,. \tag{79}$$

For an isentropic change of the state of the mixture of t non-ideal gas and small solid particles, under the thermodynamic equilibrium condition, we may calculate the equilibrium sound speed in the mixture, as follows

$$a_m = (\frac{\partial p}{\partial \rho})_S^{1/2} = \left[\frac{\{\Gamma+(2\Gamma-Z)b\rho(1-K_p)\}p}{(1-Z)\rho\{1+b\rho(1-K_p)\}}\right]^{1/2} \tag{80}$$

neglecting $b^2\rho^2$, where subscript 'S' refers to the process of constant entropy.
The adiabatic compressibility of the mixture of the non-ideal gas and small solid particles can be calculated as (c. f. [40])

$$C_{adi} = -\rho\left(\frac{\partial}{\partial p}\left(\frac{1}{\rho}\right)\right)_s = \frac{1}{\rho a_m^2} = \frac{(1-Z)\{1+b\rho(1-K_p)\}}{\{\Gamma+(2\Gamma-Z)b\rho(1-K_p)\}p} \quad (81)$$

Using the equations (46), (47) and (49) in the equation (81), we get the non-dimensional expression for the adiabatic compressibility as

$$(C_{adi})P_a = \frac{(1-Z_aD)1+\bar{b}D(1-K_p)]}{[\Gamma+\bar{b}D(1-K_p)(2\Gamma-Z_aD)]\gamma M^2 P} \quad (82)$$

Also, the total energy of the flow field between the piston and the cylindrical shock wave is given by

$$E = 2\pi\int_{r_p}^{R}\rho\left[\frac{1}{2}(u^2+v^2+w^2)+U_m-\bar{G}m\right]rdr, \quad (83)$$

where r_p is the radius of the piston or the inner expanding surface . Now by using the similarity transformations (43) to (50) and the equations (52) and (53) in the relation (83), we get

$$E = 2\pi\rho_a R^4 Q^2 J, \quad (84)$$

Where

$$J = \int_{\eta_p}^{1} D[\frac{(U^2+V^2+W^2)}{2}+\frac{P(1-Z_aD)}{(\Gamma-1)[1+\bar{b}D(1-K_p)]}-G_0S]\eta d\eta, \quad (85)$$

η_p being the value of 'η' at the piston or inner expanding surface.

Equation (84) show that the total energy of the flow field behind the cylindrical shock wave is proportional to the fourth power of the shock radius R. This increase can be achieved by the pressure exerted on the fluid by the inner expanding surface (a contact surface or a piston). The situation of the similar type may prevail in the formation of cylindrical spark channels from exploding wires. In addition, in the usual cases of spark break down, time dependent energy input is a more natural assumption than the instantaneous energy input ([39, 41]). It is also dependent on the gravitation parameter G_0 ([30, 42–46]).
The ordinary differential equations (62)-(68) with boundary conditions (69)-(75) can now be numerically integrated to obtain the solution for the flow behind the shock surface.
Normalizing the variables u, v, w, ρ, p, m and F with their respective values at the shock, we obtain

1. $\frac{u}{u_n} = \frac{U(\eta)}{U(1)}$
2. $\frac{v}{v_n} = \frac{V(\eta)}{V(1)}$

3. $\frac{w}{w_n} = \frac{W(\eta)}{W(1)}$
4. $\frac{\rho}{\rho_n} = \frac{D(\eta)}{D(1)}$
5. $\frac{p}{p_n} = \frac{P(\eta)}{P(1)}$
6. $\frac{m}{m_n} = \frac{\Omega(\eta)}{\Omega(1)}$
7. $\frac{F}{F_n} = \frac{\phi(\eta)}{\phi(1)}$

3. Results and Discussion

For the existence of similarity solution of the present problem, the following conditions must be satisfied

$3q + 2\delta + s + 1 = 0,$ and $\lambda = \sigma = 1.$

From equation (22), when $\lambda = 1$, the initial angular velocity A_a remains constant. This implies that the similarity solution for the present problem is valid under conditions of variable azimuthal and axial fluid velocity while maintaining a constant angular velocity. The total energy within the flow field behind the cylindrical shock wave is not conserved but instead scales with the fourth power

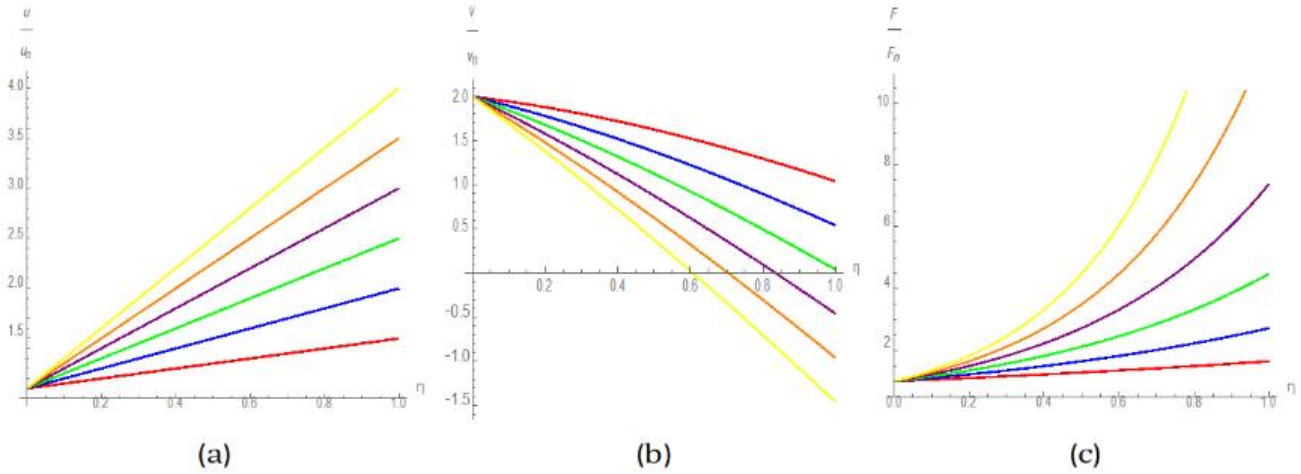

FIG. 1. Distribution of the reduced flow variables: (a) radiation flux, (b) azimuthal component of fluid velocity, and (c) radiation flux for parameter values $\alpha = -0.5$, $\delta = -1$, $q = 0$, $s = 1$, and $G_0 = 1$. Different colors represent the following cases in the region behind the shock front: 1. **Red**: $K_p = 0$, $\bar{b} = 0$ (perfect gas) 2. **Blue**: $K_p = 0$, $\bar{b} = 0.05$ (non-ideal gas) 3. **Green**: $K_p = 0$, $\bar{b} = 0.1$ (non-ideal gas) 4. **Purple**: $K_p = 0.2$, $\bar{b} = 0$, $G_a = 50$ 5. **Orange**: $K_p = 0.2$, $\bar{b} = 0.05$, $G_a = 50$ 6. **Yellow**: $K_p = 0.2$, $\bar{b} = 0.1$, $G_a = 50$

These variations illustrate the impact of gas properties on the flow behavior behind the shock front.

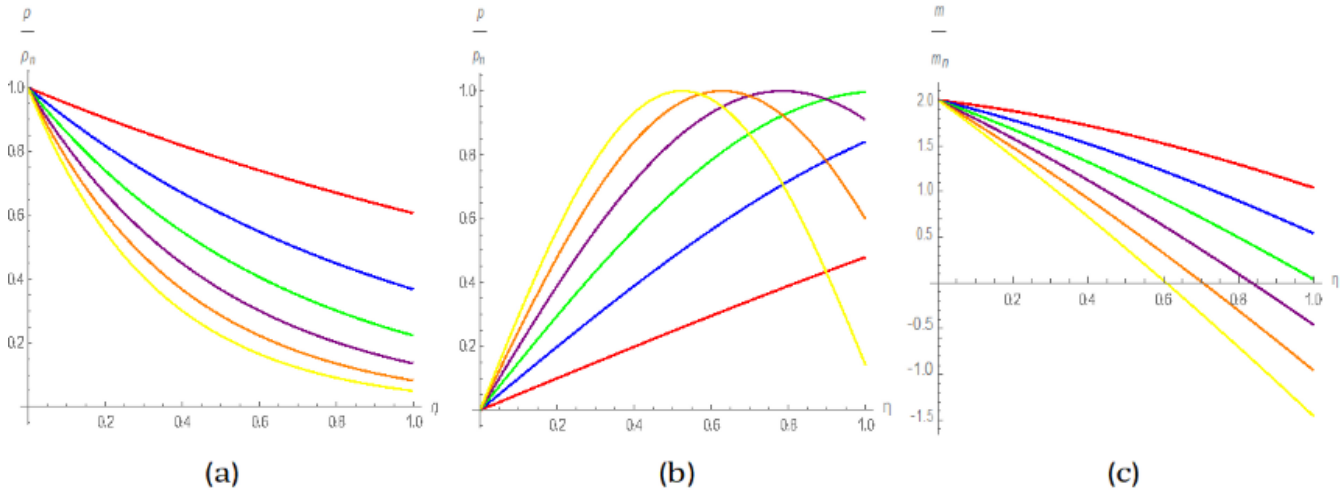

FIG. 2. Distribution of the reduced flow variables: (a) radiation flux, (b) pressure, and (c) mass for parameter values $\alpha = -0.5$, $\delta = -1$, $q = 0$, $s = 1$, and $G_0 = 1$. Different colors represent the following cases in the region behind the shock front: 1. **Red**: $K_p = 0$, $\bar{b} = 0$ (perfect gas) 2. **Blue**: $K_p = 0$, $\bar{b} = 0.05$ (non-ideal gas) 3. **Green**: $K_p = 0$, $\bar{b} = 0.1$ (non-ideal gas) 4. **Purple**: $K_p = 0.2$, $\bar{b} = 0$, $G_a = 50$ 5. **Orange**: $K_p = 0.2$, $\bar{b} = 0.05$, $G_a = 50$ 6. **Yellow**: $K_p = 0.2$, $\bar{b} = 0.1$, $G_a = 50$ These variations illustrate the impact of gas properties on the flow behavior behind the shock front.

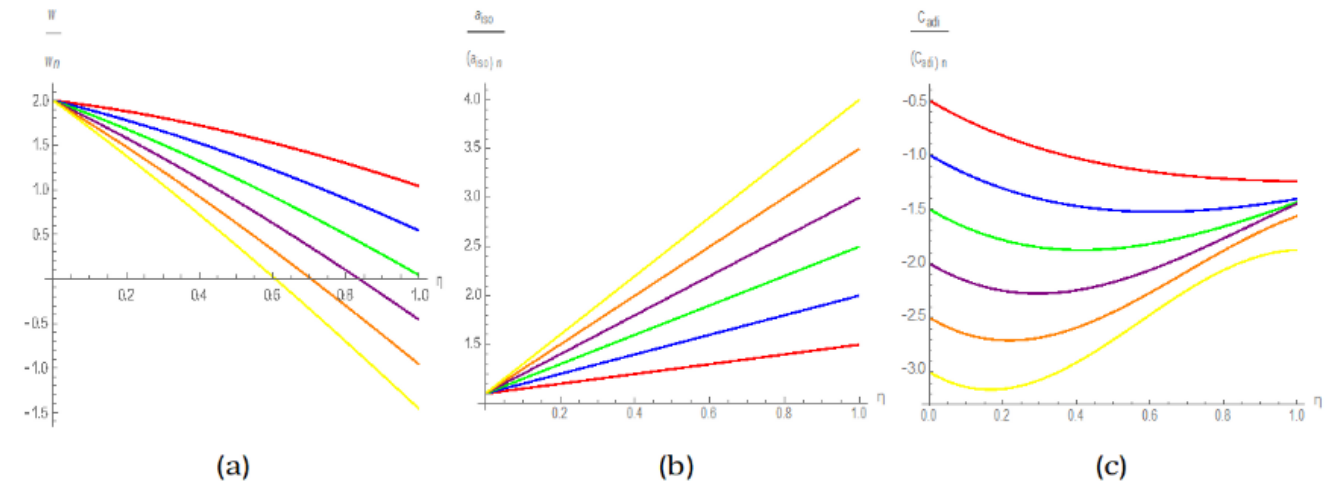

FIG. 3. Distribution of the reduced flow variables: (a) radiation flux, (b) isothermal speed of sound, and (c) adiabatic compressibility for parameter values $\alpha = -0.5$, $\delta = -1$, $q = 0$, $s = 1$, and $G_0 = 1$. Different colors represent the following cases in the region behind the shock front: 1. **Red**: $K_p = 0$, $\bar{b} = 0$ (perfect gas) 2. **Blue**: $K_p = 0$, $\bar{b} = 0.05$ (non-ideal gas) 3. **Green**: $K_p = 0$, $\bar{b} = 0.1$ (non-ideal gas) 4. **Purple**: $K_p = 0.2$, $\bar{b} = 0$, $G_a = 50$ 5. **Orange**: $K_p = 0.2$, $\bar{b} = 0.05$, $G_a = 50$ 6. **Yellow**: $K_p = 0.2$, $\bar{b} = 0.1$, $G_a = 50$ These variations illustrate the impact of gas properties on the flow behavior behind the shock front of the shock radius. The variation of flow variables between the shock front ($\eta =$

1) and the inner expanding surface or piston ($\eta = \eta_p$) is determined through numerical integration of equations (62)-(68), subject to boundary conditions (69) to (75). This integration is performed using the fourth-order Runge-Kutta method. The constant parameter values considered for this study are $\gamma = 1.4$; $K_p = 0, 0.2, 0.4$; $G_a = 50, 100$; $\beta' = 1$; $\bar{b} = 0, 0.05, 0.1$; $M^2 = 25$; $G_0 = 0.25, 1, 5, 10, 20$;

and $w^*/Q = 0.005$, $\xi = 0.1, 1, 10, 50$. The values $\gamma = 1.4$ and $\beta' = 1$ correspond to a mixture of air and glass particles, as described in Miura's study. The shock Mach number M = 5 is selected to model the flow of a non-ideal gas and pseudo-fluid (small solid particles) in velocity and temperature equilibrium. The case $K_p = 0$ represents a dust-free environment, while $K_p = 0$ and $\bar{b} = 0$ correspond to an ideal gas scenario. The density ratio β across the shock front, the shock strength $(1 - \beta)$, and the position of the inner expanding surface or piston η_p are evaluated for various values of K_p, G_a, $\bar{b}$, ξ, and G_0. The results are documented accordingly.

Figures 1, 2 and 3 illustrate the variations in the reduced flow variables u/u_n, v/v_n, ρ/ρ_n, p/p_n, m/m_n, F/F_n, and the reduced adiabatic compressibility $C_{adi}/(C_{adi})_n$ with respect to η for different parameter values while keeping other constants fixed. The trends in these figures indicate that as the radial distance increases from the inner expanding surface (piston) toward the shock front, the radial velocity component u/u_n, density ρ/ρ_n, pressure p/p_n, mass m/m_n, total heat flux F/F_n and adiabatic compressibility $C_{adi}/(C_{adi})_n$ also increase. Increasing the value of the non-idealness parameter $\bar{b}$ leads to the following effects: 1. A decrease in shock strength.

2. An increase in the distance between the piston and the shock front.
3. A decrease in flow variables u/u_n, ρ/ρ_n, p/p_n, F/F_n.
4. An increase in flow variables $\frac{v}{v_n}$, $\frac{w}{w_n}$, $\frac{m}{m_n}$, $\frac{C_{adi}}{(C_{adi})_n}$

These effects can be explained physically as follows: A higher value of $\bar{b}$ increases the compress- ibility of the medium, leading to an increased distance between the shock front and the piston, reduced shock strength, and the observed behavior of the flow variables.
Increasing the mass concentration of solid particles K_p results in:

1. An increase in shock strength.
2. A decrease in the distance between the piston and the shock front.
3. A decrease in flow variables u/u_n, v/v_n, m/m_n, $(C_{adi})/(C_{adi})_n$.
4. An increase in flow variables ρ/ρ_n, p/p_n, F/F_n.

Physically, small solid particles with density equal to or greater than that of the gas occupy more volume, reducing the medium's compressibility. As K_p increases, compressibility further decreases, leading to a change in shock strength and flow variable behavior.
The impact of increasing G_a includes:

1. An increase in shock strength.

2. A decrease in the distance between the piston and the shock front.
3. Negligible effects on flow variables u/u_n, v/v_n, $(C_{adi})/(C_{adi})_n$.
4. For $K_p = 0.2$, negligible effects on w/w_n, ρ/ρ_n, p/p_n, m/m_n, F/F_n, $a_{iso}/(a_{iso})_n$.
5. For $K_p = 0.4$, a decrease in w/w_n, m/m_n, $a_{iso}/(a_{iso})_n$, and an increase in ρ/ρ_n, p/p_n, F/F_n, $l_\theta/l_{\theta n}$.

At higher values of K_p, these effects become more pronounced. As G_a increases while K_p remains constant, the volume fraction of solid particles in the undisturbed medium decreases. This enhances compression between the shock and the expanding surface, leading to the observed effects. Increasing ξ causes:

1. An increase in the distance between the piston and the shock front.
2. Negligible effects on u/u_n, ρ/ρ_n, p/p_n, m/m_n, $(C_{adi})/(C_{adi})_n$.
3. A decrease in radiation heat flux F/F_n. The effect of ξ dominates over other dusty gas parameters such as $\bar{b}$, K_p, and G_a for values between 1 and 50. For $\xi = 10$ and 50, the radiation flux increases rapidly near the shock front.

These effects indicate that higher values of ξ result in greater absorption of monochromatic radiation by the gas in the flow-field behind the shock front. The shock strength remains unchanged. An increase in G_0 leads to:

1. A decrease in the distance between the piston and the shock front.
2. An increase in flow variables u/u_n, ρ/ρ_n, p/p_n, F/F_n.
3. A decrease in flow variables v/v_n, w/w_n, m/m_n, $(C_{adi})/(C_{adi})_n$.

The shock strength remains constant. Since $G_0 = \frac{\bar{G}\pi\rho\bar{a}}{Q}2$is inversely proportional to Q, which is

proportional to the shock velocity $\dot{R}$, an increase in G_0 reduces $\dot{R}$. Also, the piston position η_p is inversely proportional to $\dot{R}$, so η_p increases with G_0, reducing the distance between the piston and the shock front. As G_0 increases, compressibility decreases, resulting in the observed variations in flow variables.

4. Conclusions

This study examines the self-similar flow behind a cylindrical shock wave propagating through a rotating, axisymmetric mixture of a non-ideal gas and small solid particles, influenced by monochro- matic radiation and a gravitational field. The analysis considers varying fluid velocities and as- sumes an initially constant density. The findings provide insight into the impact of key parame- ters—including the non-idealness parameter, the mass concentration of solid particles, the density ratio of solid particles to the gas, the radiation parameter, and the gravitational parameter—on both the shock strength and the flow field behind the shock front. The similarity solution exists only under specific conditions, where the radiation exponent q is related to the pressure exponent δ, the position exponent s, and the time exponent l in the radiation absorption coefficient, satisfying the relations $3q + 2\delta + s + 1 = 0$ and $s + l = -1$. Additionally, the azimuthal fluid velocity exponent λ must equal the axial fluid velocity exponent σ, both having a value of 1. Under these conditions, the initial angular velocity remains constant.

The effects of the radiation parameter ξ on the variation of flow variables are generally negligible, except for its influence on radiation heat flux, where it plays a dominant role over the dusty gas parameters in determining variations behind the shock front. Furthermore, the total energy within the flow field behind the shock wave is not conserved but is instead proportional to the fourth power of the shock radius R. Shock strength remains unaffected by the radiation parameter ξ and the gravitational parameter G_0, but it is influenced by the dusty gas parameters $\bar{b}$, K_p, and G_a. The distance between the piston and the shock front increases with higher values of the radiation parameter ξ, the non-idealness parameter $\bar{b}$, and the mass concentration of solid particles K_p, while it decreases with an increase in the density ratio of solid particles to gas G_a and the gravitational parameter G_0

References:

1. S.I. Pai, S. Menon and Z.Q. Fan, Similarity solution of a strong shock wave propagation in a mixture of a gas and dust particles, Int. J. Eng. Sci. 18, 1365-1373, 1980.
2. F. Higashino and T. Suzuki, The effect of particles on blast wave in a dusty gas, Z. Naturforsch. A 35, 1330-1336, 1980.
3. H. Miura and I.I. Glass, Development of the flow induced by a piston moving impulsively in a dusty gas, Proc. R. Soc. A 397, 295-309, 1985.
4. H. Miura, Decay of shock waves in a dusty gas shock tube, Fluid Dyn. Res. 6, 251-259, 1990.
5. W. Gretler and R. Regenfelder, Strong shock wave generated by a piston moving in a dust-laden gas under isothermal conduction, Eur. J. Mech. B/Fluids 24, 205-218, 2005.

6. J.S. Park and S.W. Baek, Interaction of a moving shock wave with a two-phase reacting medium, Int J Heat Mass Transf. 46, 4717-4732, 2003.
7. H. Steiner and T. Hirschler, A self similar solution of a shock propagation in a dusty gas, Eur. J. Mech. B Fluids 21, 371-380, 2002.
8. L.I. Sedov, Similarity and Dimensional Methods in Mechanics, Academic Press, New York, 1959.
9. R.E. Marshak, Effect of radiation on shock wave behaviour, Phys. Fluids 1(1), 24-29, 1958.
10. L.A. Elliott, Similarity Methods in Radiation Hydrodynamics, Proceedings of the Royal Society of London 258, 287-301, 1960.
11. K.C. Wang, The piston problem with thermal radiation, J. Fluid Mech. 20(3), 447-455, 1964.
12. J.B. Helliwell, Self-similar piston problems with radiative heat transfer, J. Fluid Mech. 37, 497-512, 1969.
13. J.R. Nicastro, Similarity analysis of the radiative gas dynamics equations with spherical symmetry, Phys. Fluids 13, 2000-2006, 1970.
14. G. Deb Ray and J.B. Bhowmick, Similarity solutions for expansions in stars, Int. J. Pure Appl. Math. 7, 96-103, 1976.
15. V.M. Khudyakov, The self-similar problem of the motion of a gas under the action of monochromatic radiation, Soviet. phys. Dokl. 28, 853-855, 1983. (Trans. Amer. Inst. of Phys.)
16. A.N. Zheltukhin, A family of exact solutions of the equations of the one-dimensional motion of a gas under the influence of monochromatic radiation, J. Appl. Math. Mech. 52, 262-263, 1988.
17. O. Nath, Propagation of cylindrical shock waves in a rotating atmosphere under the action of monochro- matic radiation, IL NUOVO CIMENTO 20D, 1845-1852, 1998.
18. O. Nath, and H.S Takhar, spherical MHD Shock waves under the action of monochromatic radiation, Astrophysics and space science, 202, 355-362, 1993.
19. S. Shinde, Propagation of cylindrical shock waves in a non-uniform, rotating stellar atmosphere under the action of monochromatic radiation and gravitation, Math. Comput. Appl. 11(2), 95-102, 2006.
20. J.P. Vishwakarma and V.K. Pandey, Self-similar flow under the action of monochromatic radiation behind a cylindrical MHD shock in a Non-ideal gas, Appl. Math. 2(2), 28-33, 2012.
21. G. Nath, P.K. Sahu and M. Dutta, Magnetogasdynamic cylindrical shock in a rotational axisymmetric non-ideal gas under the action of monochromatic radiation, Procedia Eng. 127, 1126-1133, 2015.
22. G. Nath and P.K. Sahu, Unsteady adiabatic flow behind a cylindrical shock in a rotational axisymmetric non-ideal gas under the action of monochromatic radiation, Procedia Eng. 144, 1226-1233, 2016.
23. G. Nath, P.K. Sahu, Similarity solution for the flow behind a cylindrical shock wave in a rotational axisymmetric gas with magnetic field and monochromatic radiation, Ain Shams Engineering Journal, 2016.

24. G. Nath and P.K. Sahu, Propagation of a cylindrical shock wave in a mixture of a non-ideal gas and small solid particles under the action of monochromatic radiation, Combust. Explos. Shock Waves 53(3), 59-71, 2017.
25. P.K. Sahu, Cylindrical shock waves in rotational axisymmetric non-ideal dusty gas with increasing energy under the action of monochromatic radiation, Phys Fluids. 29, 086102, 2017.
26. P. Carrus, P. Fox, F. Hass and Z. Kopal, The propagation of shock waves in a stellar model with continuous density distribution, Astrophys. J. 113, 496-518, 1951.
27. M.H. Rogers, Analytic solutions for the blast wave problem with an atmosphere of varying density, Astrophys. J. 125, 478-493, 1957.
28. Patel, A self similar flow behind a shock wave in a dusty gas under a gravitational field, J. Nat. Acad. Math. India 27, 83-98, 2013.
29. J.B. Singh, A self-similar flow in generalized Roche model with increasing energy, Astrophys. Space Sci. 88, 269-275, 1982.
30. R. Bajargaan and A. Patel, Similarity solution for a cylindrical shock wave in a self-gravitating, rotating axisymmetric dusty gas with heat conduction and radiation heat flux, J. Appl. Fluid Mech. 10(1), 329- 341, 2017.
31. R. Bajargaan and A. Patel, Self similar flow behind an exponential shock wave in a self-gravitating, rotating, axisymmetric dusty gas with heat conduction and radiation heat flux, Indian J. Phys., 2018, http://doi.org/10.1007/512648-018-1199-z.
32. V.A. Levin and G.A. Skopina, Detonation wave propagation in rotational gas flows, J. Appl. Mech. Tech. Phys. 45, 457-460, 2004.
33. H.A. Zedan, Applications of the group of equations of the one-dimensional motion of gas under the influence of monochromatic radiation, Appl. Math. Comput. 132, 63-71, 2002.
34. J.P. Vishwakarma and G. Nath, A self-similar solutions of shock propagation in a mixture of a non-ideal gas and small solid particles, Meccanica 44, 239-254, 2009.
35. S.I. Pai, Two phase flows, Vieweg tracts in pure and applied physics, Vol. 3, Ch. V (Vieweg-Verlag, Braunschweig, 1977).
36. YA. B. Zel'dovich and YU. P. Raizer, Physics of Shock Waves and High Temperature Hydrodynamic Phenomena, vol. II., Academic Press, New York, 1967.
37. M.P. Ranga Rao and B.V. Ramana, Unsteady flow of a gas behind an exponential shock, J. Math. Phys. Sci. 10, 465-476, 1976.
38. P. Rosenau, Equatorial propagation of axisymmetric MHD shocks II, Physics of Fluids, 20(7), 1097- 1103, 1977.
39. J.P. Vishwakarma and G. Nath, Similarity solution for a cylindrical shock wave in a rotational axisym- metric dusty gas with heat conduction and radiation heat flux, Commun. Nonlinear Sci. Numer. Simul. 17, 154-169, 2012.
40. E.A. Moelwyn-Hughes, Physical Chemistry, Pergamon Press, London, 1961.
41. R.A. Freeman and J. Craggs, Shock wave from spark discharges, Brit. J. Appl. Phys. 2, 421-427, 1969.
42. Nandita and R. Arora, "Approximate analytical solution using power series method for the propagation of blast waves in a rotational axisymmetric non-ideal gas," 2023.
R. Bajargaan and A. Patel, "Self similar flow under the action of monochromatic radiation

behind a cylindrical shock wave in a self-gravitating, rotating axisymmetric dusty gas," 2023.

43. R.A. Freeman and J. Craggs, Shock wave from spark discharges, Brit. J. Appl. Phys. 2, 421-427, 1969.
44. Patel, "Similarity solution for a cylindrical shock wave in a self-gravitating, rotating axisymmetric dusty gas with heat conduction and radiation heat flux," *Journal of Applied Fluid Mechanics*, vol. 10, no. 1, pp. 329–341, 2024.
45. P. K. Sahu, "Cylindrical shock waves in rotational axisymmetric non-ideal dusty gas with increasing energy under the action of monochromatic radiation," *Physics of Fluids*, vol. 29, no. 8, p. 086102, 2022.
46. G. Nath, "Self-similar solution of cylindrical shock wave propagation in a rotational axisymmetric dusty gas," *Meccanica*, vol. 47, pp. 1581–1595, 2023.